16.08.91

# Calculation Criteria and Application of "Rollgurt"-Conveyor (Tube Conveyor)

## 1. Introduction

In recent years, conveyor belts have penetrated completely new fields, particularly where the location of routes is extremely difficult, where these have to go uphill and down dale and have to overcome curves while at the same time transporting bulk solids in a steady flow. As a result of the ever increasing demand for higher output combined at the same time with more universal possibilities of application the trend of development is for an increase of the handling speed from 5,5 m/s to 8,0 m/s for a better degree of utilization (filling degree) of the belt by shaping of the troughed belt, through the box-type belt to the tubular belt and to the adaptation of the belt system to the topographic conditions, from the horizontal conveying to the steep and vertical conveying.

In many industrial production sectors such as coal fired power stations, cement plants or steelmaking plants, special attention must be paid nowadays to environmental protection. From this point of view the tube type conveyor has been introduced and in the meantime fully accepted by the industry.

The major advantages of the Tube Conveyor are:

- The material within the tube is effectively protected from the element and from contamination;

- Dust is effectively controlled and even the immediate vicinity of the belt is dust-free, an important point for maintenance and operating staff. Since it is not necessary to encase the conveyor in a cover-type structure;

- The cross section required by a Tube Conveyor installation is considerably less than that of a conventional conveyor. A lighter support structure is also feasible;

- One of the major causes of premature belt wear in a conventional belt conveyor such as tracking problems causing edge damage, is largely eliminated.

Tube Conveyors designed to date include belt diameters ranging from 100 to 800 mm, the capacities ranging from 40-2.000 $m^3$/h and are operated at speeds comparable with conventional belt conveyors.

A number of various designs as shown in Fig. 1 has been introduced.

Based on operational experience made so far, PWH/Continental developed the "Rollgurt" Conveyor (Fig. 2). The special features and advantages of this system are as follows:

- The tension carriers of the rolled belts are arranged in the overlapping edge zones (Fig. 3). Therefore the tension carrier, being the part of the belt with the smallest elongation in length, will tend to select with a curved belt route always the shortest way, i.e. will run in the inside radius. This means that when the Rollgurt is running through curves the overlapping belt edges, because of the belt tension, will be pressed firmly against the inner idler of the idler chair.
  **Advantage:**
  As a result thereof is obtained a good sealing of the rolled belt.

- By the location of the tension carriers in the overlapping zones is furthermore ensured that in a curve the bulgy outer part of the belt is relatively soft and therefore well flexible.
  **Advantage:**
  Thus are obtained close curve radii. Curves up to 165 x d could already be designed (usually 300 x d).
  d = rolled-in diameter.

- In the curves the settable idlers stations are aligned, following the natural run of the belt, so that in the idler station is always ensured an equal position of the Rollgurt.
  **Advantage:**
  Smooth steady run of the belt without tumbling movements.

- In the idler stations the idlers are arranged in a way (Fig. 4) that, when running through these stations, the Rollgurt does not have an all circular shape, but an elliptic one. Thus the position of the Rollgurt is better fixed in the idler stations and the run of the Rollgurt is steadier.
  **Advantage:**
  Smooth steady belt run of the belt without tumbling movement, also on the straight lengths of the belt route.

- The 6 idlers in each idler station are here arranged in such a way (Fig. 5) that the shell surfaces of the idlers form an enclosed polygon. It is thus prevented that with its edges the belt could run laterally against the idlers.
  **Advantage:**
  Protection of the belt edges against higher wearing.

## 2. Calculation Criteria for Tube Conveyors

Although a number of tube conveyors have been designed and are in operation since years worldwide, there is so far no standard available for calculations of power consumption, friction values, belt tensions, material load, etc.

The international standard DIN 22 101 / ISO 5048 for calculations of Belt Conveyors with carrying idlers does not cover the specific criteria of the tube conveyor. However, the basic parameters and calculation formulae for determining belt forces and operating power requirements can be adapted.

In detail the following motion resistances are valid for the "Rollgurt" Conveyor:

| | |
|---|---|
| 1. Main resistances | - rotational resistance due to friction in the idler bearings<br>- belt advancement resistance |
| 2. Secondary resistances | - inertial and frictional resistances due to acceleration<br>- resistance due to friction at the loading area<br>- pulley bearing resistance<br>- resistance due to wrapping of the belt on the pulleys |
| 3. Special main resistances | - drag resistance due to forward tilt of the idler |
| 4. Special secondary resistances | - resistance due to friction with belt and pulley cleaners |
| 5. Slope resistance | - resistance due to lifting or lowering the material on inclined and/or declined conveyor routes |

Additional resistances resulting from the tube conveyor design such as horizontal and vertical curve friction, tube forming resistance, etc. can be accommodated in the main resistance and calculated in a simplified manner by using an artificial friction coefficient

$f_{Rollgurt}$ as adapted to ISO 5048.

The calculation of the required peripheral force $F_u$ on the driving pulley will be carried out with the known formula

$$F_u = f_R \cdot L \cdot g \; (q_{Ro} + q_{Ru} + (2q_B + q_G)\cos\delta\;) + \sum F_N \pm q_G \cdot H \cdot g$$

| Symbol | Unit | Description |
|---|---|---|
| $f_R$ | - | artificial friction coefficient for "Rollgurt" |
| L | m | conveyor length |
| g | m/s | acceleration due to gravity |
| $q_{Ro}$ | kg/m | mass of carrying side revolving idler parts |
| $q_{Ru}$ | kg/m | mass of returnside revolving idler parts |
| $q_B$ | kg/m | mass of belt |
| $q_G$ | kg/m | mass of material |
| | | slope angle of the conveyor route |
| $F_N$ | N | additional resistances |
| H | m | lift of conveyor |

In practice it has been proven that this procedure is sufficient as long as the specific friction value $f_R$ is known.
Therefore test runs in the test field as well as in practice are necessary to obtain reliable results.

## 3. Tests on Power Consumption and Friction Loss of a "Rollgurt" Conveyor in a Cement Plant

The built "Rollgurt" Conveyor (Fig. 6) is the Transport Connection for pre-dried lime between the Lime Preparation Plant and the new Furnice Line with a capacity of 90 t/h, a centre distance of 385 m and a lift of 14 m. At a belt width of 730 mm and an idler spacing of 1,5 m the tube diameter is 200 mm. The "Rollgurt" passes through an S-curve with radius 60 to 100 m and a vertical curve of radius 200 m with an idler spacing of 1,0 m or resp. 1,3 m. The broken and pre-dried lime has a residual moisture of 10 to 15 % at a temperature of 30 to 60 degrees Celsius, a lump size of 0 to 80 mm and an apparent density of approx. 1,1 t/cu.m. The material with a fines portion 1.0 mm of approx. 20 % has bad flowing characteristics and tends, in particular at the transfer points, to clog.

With field measurements at the "Rollgurt"-Conveyor used in the lime and cement works Alsen-Breitenburg in Germany motional resistances had been determined for various loads. During these measurements the following data had been determined:

| | |
|---|---|
| Overall plant: | mass flow<br>pre-tensional force<br>drive pulley torque<br>driving power<br>belt speed |
| Carrying belt run: | normal and horizontal forces for each idler as well as vertical and horizontal force for each complete station at<br>- straight belt route<br>- curved route<br>and varying loads |

Return belt run: normal and horizontal forces for each idler as well as vertical and horizontal force each complete station at
- straight belt route
- curved route
and varying loads

The following measuring variables have been determined:

| | |
|---|---|
| - drive pulley torque | M |
| - belt speed | v |
| - electric effective drive power | $P_{el}$ |
| - belt weigher signal | m |
| - vertic. force at measuring idler ring | $F_v$ |
| - horiz. force at measuring idler ring | $F_h$ |
| - normal force measuring idler no. 1 | $R_{n1}$ |
| - horiz. force measuring idler no. 1 | $R_{h1}$ |
| - normal force measuring idler no. 2 | $R_{n2}$ |
| - horiz. force measuring idler no. 2 | $R_{h2}$ |
| - normal force measuring idler no. 3 | $R_{n3}$ |
| - horiz. force measuring idler no. 3 | $R_{h3}$ |
| - normal force measuring idler no. 4 | $R_{n4}$ |
| - horiz. force measuring idler no. 4 | $R_{h4}$ |
| - normal force measuring idler no. 5 | $R_{n5}$ |
| - horiz. force measuring idler no. 5 | $R_{h5}$ |
| - normal force measuring idler no. 6 | $R_{n6}$ |
| - horiz. force measuring idler no. 6 | $R_{h6}$ |

The measuring data had been registered and stored by a digital measuring data logger with a scanning frequency of 5 HZ.

Measuring Results

The forces acting in normal and in horizontal direction on to the individual idlers are shown in polar diagrams and in histograms (so that figures can be read more easily) (Fig. 7). For the carrying belt run have always been recorded the forces with varying mass flows and for the return belt run the average, the maximum and the minimum forces.

In the polar diagrams is shown each time the amount of force in direction to the respective idler. The coordinates' system is always directed thus that it corresponds to the view on to an idler ring in direction of handling of the carrying belt run. The measuring idler at the measuring point position 90 degrees is always the upper idler, the one at the measuring point position 270 degrees is always the lower idler. In the picture are shown the normal forces $R_n$ acting on to the measuring idlers in the carrying belt run in straight line with their amount and direction. It is visible that with this example no normal force is acting on to the measuring idlers at the measuring point positions 30 degrees and 150 degrees; i.e. at these angles the "Rollgurt" is not contacting the idlers. On to the measuring idlers at the measuring point positions 210 degrees, 270 degrees and 330 degrees are acting mostly forces as resulting from the belt weight and the loads, whereas on to the measuring idlers at position 90 degrees, where the overlapping with the tension carriers is contacting, are only acting the forces for closing the belt. In the diagram are only shown the normal forces $R_n$, by arrows, for a loading of 71 t/h. The dotted lines show the lengths of the vectors with low mass flows.

In picture 8 are combined the same polar diagram and the corresponding histogram. The four different loading situations are identified by differing symbols and shown in the legend. The end points of the vectors are connected by lines, so that the attribution of the points is facilitated. In the histogram is outlined once more the normal force $R_n$ in N for the various measuring point positions and loads, so that the values in figures can be read more easily. At the measuring position 30 degrees and 150 degrees the normal force is zero. Stronger lines have been selected for the histograms of the empty belt than for the loads situations for emphasizing this special load case. Whereas with empty belt the normal forces on to the measuring idlers at the positions 210 degrees, 270 degrees and 330 degrees are smaller than for the loaded belt, the normal force becomes greater with no-load run for the upper idler (measuring point position 90 degrees).

Figure 9 shows the normal and the horizontal forces on to the measuring idlers in the carrying belt run in straight line by way of polar diagrams and histograms. Here are shown the data for four different mass flows. In the upper diagram are each shown the normal forces $R_n$ and in the lower one the horizontal forces $R_h$ acting on to the individual measuring idlers. Furthermore should be considered the different scales of the axes that at the ration of 10:1 are also reflecting the interrelation of the forces.

With overfilling of the "Rollgurt" resulted the following situation:
The then measured normal and horizontal forces on to the measuring idlers are shown in picture 10 in addition to the forces measured at the empty belt and the forces measured with the mass flow 71 t/h. In particular should be considered the much smaller scale of max. 800 N resp. 80 N compared to the previous pictures. Although the mass flow increase was only 17 %, the forces on the measuring idlers increased by more than 150 %! The constraining forces that occur here are also manifesting by the fact that now normal forces can be measured at all of the idlers.

Forces in the Carrying Belt Run in the Curve

In picture 11 is shown the normal and the horizontal forces on to the measuring idlers in the carrying belt run in the curve for three different mass flows. The total idler ring is turned in the horizontal curve through 9 degrees to the right; therefore the measuring point position 270 degrees does not correspond in this case to an idler arranged perpendicularly under the belt.

At the measuring idlers of the measuring point position 90 degrees and 150 degrees the "Rollgurt" is not in contact. The greatest forces occur at the 30 degrees' position, as there is the overlapping zone of the "Rollgurt" with the tension carriers. The normal and horizontal forces that both are considerably higher compared to those of a straight line result from the belt tensional force in the "Rollgurt". The additional forces resulting from loading are relatively small.

Forces in the Return Belt Run on the Straight Line

In picture 12 is shown the normal and the horizontal forces on the individual measuring idlers in the return belt run on the straight line. These forces don't depend upon the loading of the carrying belt run; they are fluctuating, however, in the course of one belt circulation between maximum and minimum.

The pictures show a rather uniform distribution of forces on to the idlers. When the measuring was made the overlapping was at the measuring point position 90 degrees, although with nontorsioned return belt run it should be in the position 270 degrees; the overlapping is always only a very short time in contact with the measuring idler. The average values shown by the thicker line outline the average force during one whole belt circulation.

Forces in the Return Belt Run in the Curve

In picture 13 is shown the normal and the horizontal forces on to the individual measuring idlers in the return belt run in the curve. The much bigger forces act on to the measuring idler at the measuring point position 330 degrees, where the overlapping zone is contacting the idler with the tension carriers. These are resulting from the belt tensional force in the "Rollgurt". The average values of the forces during one belt circulation are again marked by the greater thickness of the line. As already described before maximum and minimum forces are average values of timely intervals within one circulation.

Quotient from Horizontal and Vertical Force at the complete Idler Ring

In picture 14 is shown the quotient from horizontal and vertical force at the complete idler ring as a function of the vertical force for all measuring points. With increasing loading the quotient for the carrying belt run approximates the value 0.22. For the return belt run result somewhat lower values, i.e. 0.14 on the straight line or 0.21 in the curve. With a smaller vertical force (empty belt) the quotient is higher than with the loaded belt. The two individual black points result from the high horizontal forces as resulting with overfilling of the "Rollgurt".

**Evaluation of the Data measured at the Drive Unit**

Driving Torque M

The driving torque is shown in picture 15 as a function of the mass flow. It increases progressively with the mass flow.

Mechanical Driving Power $P_m$

The mechanical driving power is calculated from the belt speed, the driving torque and the drive pulley diameter. The belt speed is 1.26 and is constant, independent of the load.
Thus is resulting the driving power shown in picture 16 over the mass flow as the product of the driving torque with a constant factor.

Electric Effective Power $P_{el}$ at the Drive Motor

The electric effective power is shown in picture 17 as a function of the mass flow. Its graph is nearly in parallel to the mechanical power. The drive motor has a rated capacity of 55 kW as is also necessary with a mass flow of approx. 80 t/h. In picture 18 the electric effective power is shown over the mechanical driving power. A linear interrelation of the powers is evident.

Within the scope of field measurements at a "Rollgurt"-Conveyor in the lime and cement works Alsen-Breitenburg have been determined the normal and the horizontal forces acting on to the idlers and idler rings at four different measuring locations as well as the powers and torques occurring at the drive system. It then became evident that the forces required for shaping and guiding the "Rollgurt" are considerable compared to the forces resulting from the loading and the belt weight. The horizontal forces are attributable to only a small extent to the idler running resistance that had been measured in the laboratory. Instead it is mainly the squeezing resistance that is responsible for the high horizontal forces and the driving power resulting thereof.

The tube-conveyor is sensitive to volumetric overfilling. Already a small increase of the volume flow beyond the rated volume flow results in a considerable increase of the forces and hence of the required driving power. Therefore overfilling should be avoided if any possible.

Based on the measured data an $f_R$-value can be determined for the "Rollgurt", for thus being able to apply the ISO 5048-formulae. For ensuring the measured data certainly another series of measurements will still be necessary similar to those having been made for the conventional belt conveyor systems.

## 4. Control Mechanism for an optimized "Rollgurt" Conveyor Operation

Due to the number of criteria like vertical and horizontal curves, tube diameter, speed, material load configuration along the conveyor route, varying ambient temperatures and friction values special control mechanism of drives and pretension device are of advantage for an optimized conveyor operation. Especially in the field of tube conveyors with uncertain parameters during operation regarding friction values a new thinking of control philosophies is advantageous to minimize the costs of the valuable elements like the belting.

It would be advantageous, for reducing the belt tensional forces, to use regulated drive systems, as then the high peak loads of the belt, as would occur with unfavourable operation and loading situations, can be avoided. With the aid of variable drive units, as e.g. frequency-controlled three-phase asynchronous motors or with three-phase asynchronous motors along with variable fluid couplings, there is the possibility to limit the driving moment in a suitable way, so that during the operation phase of the conveyor system no unnecessarily high belt tensional forces will occur.

When rating and dimensioning the plant special attention should be paid to the greatest possible reduction of the pretension force T2 and the driving force F. The total driving force F can, by a suitable distribution to several drive units at different points, be kept locally relatively small, so that thereof results again a small pretension force T2 for allowing a slipfree transmission of power.

The belt tension force level is therefore smaller compared with an individual pulley drive.

When the values T2 and F and therefore T1 are being fixed with the help of a calculation schedule, then these data must not only comply with stationary, but also with instationary operation conditions, as e.g. starting and braking of the plant. Furthermore other parameters are to be considered in the calculations, such as partial loading situations (Fig. 19) of the plant and also fluctuations of the friction-affected resistance forces, so that finally the belt conveyor system can be operated smoothly and free of any trouble. This necessitates, however, that the belt is rated for the most unfavourable case.

Here, fully new control engineering strategies are adopted for considering changes or variations of operation. As a result of the control engineering measures belts of lower strength can be used compared to conventional rating criteria.

The control strategy is based here on the principle of a plant self-identification.

The determining value for rating a belt conveyor system is the plant resistance force F that is composed mainly of a friction-affected portion and a lifting portion.

The lifting portion can be determined theoretically with sufficient accuracy, whereas the friciton-affected portion is based on assumptions of the friction coefficient f that can be subjected to a fluctuation factor up to 5 and is influencing in the same way the belt force level of the plant. To date this fact had been considered, when a plant had to be designed, by basing on the most unfavourable case, whereas nowadays with new simulation calculations the friction portion is varied. Hereof results a data field for the drive and pretension forces that is attributed to the different assumed friction values. This is overlaid furthermore by variations of loading situation and change of operation mode.

Decisive for optimizing the pretension force and the split-up of the total driving power is the knowledge of the fact that the complete plant resistance is composed of a friction portion and of a lifting portion (Fig. 20).

As an example could be taken that the total plant resistance with a certain laoding situation consists of a 30 % lifting portion and of a 70 % friction portion, or, at the same loading situation, of a 10 % lifting portion and 90 % friction portion with the same total plant resistance.

With such constellation there is a considerable variation of the friction coefficient f, so that in case no. 1 the driving must come mainly from a head and drive, whereas in the case no. 2 and 3 it must be generated by the tail end drive in order to obtain a minimum belt tension force level.

As a result of such simulation calculations we get for a number of loading situations and friction value variations the corresponding drive force break-up and value of the pretension force, so that on this basis can be determined the belt manufacture.
With the operation of a belt conveyor plant must then be adopted the control strategy that had been found with the help of the simulation computer.

Suitable power recorders at the drive units give the information with respect to the total plant resistance F, in which case, however, it doesn't become evident out of which portions of friction resistance and lifting resistance this total plant resistance is composed.

A measuring data transducer detects the actual material load $M_L$ of the conveyor system and in addition a sliding register makes it possible to determine the load distribution on the plant. Thus is fixed the lifting portion $H \cdot M_L \cdot g$ of the total plant resistance, so that now the actual friction portion or resp. friction coefficient can be found by calculation.

$$f_R = \frac{F \mp H \cdot M_L \cdot g}{C \cdot L \cdot (M_R + 2\, M_G + M_L) \cdot g}$$

In a Microprocessor fed with the respective software is now made the optimum split-up of the driving power to the individually controllable drive units. At the same time the volume of the belt pretensional force is being regulated for ensuring a slipfree transmission of the forces between drive pulley and belt.

In case, in the course of the plant operation, e.g. because of changes of temperature and wearing, the friction coefficient $f_R$ would change, this would be identified and the plant be set respectively as described above.

The theoretical calculation of the plant made in the project phase on a simulation computer is thus continued to a certain extent during the plant operation for running the machine always on the pre-calculated low belt tension level.

Compared with conventional calculation methods result with the simulation calculation costs advantages for the "Rollgurt" but also with conventional long-distance belt conveyor systems between 10 % and 30 %, depending on the plant's configuration.

It becomes evident that with the application of such control strategies and when adopting microprocessors, the plants can be built as much lighter constructions, and can lead the classical mechanical engineering from the heavy construction to light-weight construction methods, and that in particular with the "Rollgurt"-conveyor can be yielded lower investment costs than in the past.

**Summary**

The tube conveyor has been introduced nowadays in a wide field of industrial sections due to its flexible design and environmental advantage as compared with the conventional troughed belt conveyor system.

Calculation standards are not available so far, however, with a number of tests on existing plants more accurate friction values can be gathered and be adapted to ISO 5048 formulae.

New control mechanisms applied on drives and prevention device lead to an optimized system having minimum investment costs for the "Rollgurt" Conveyor.

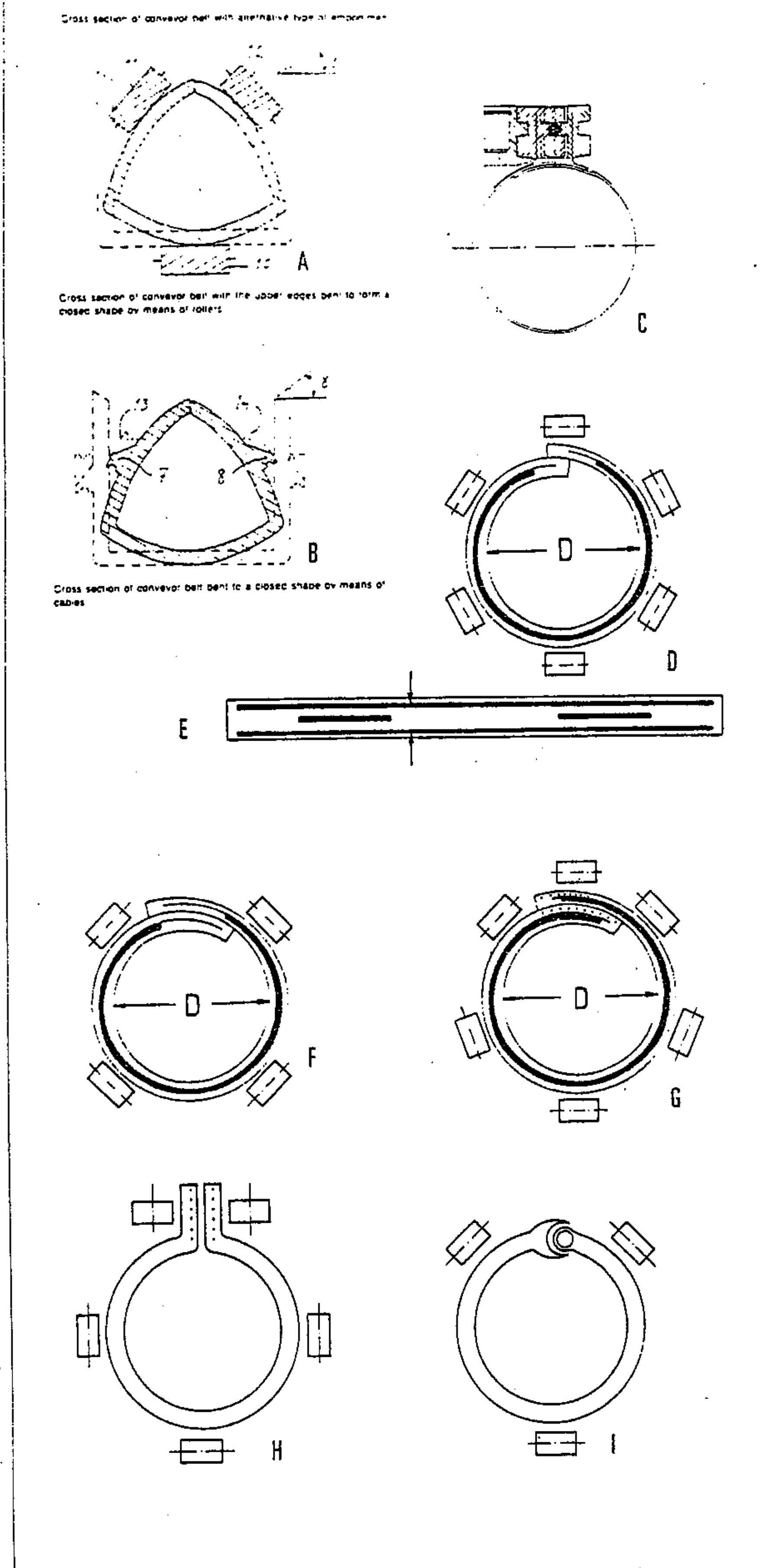


Fig.1 Cross-section of conveyor belt with alternative shapes of closed parts of belt-edges (Tube-, pipe- and hose-conveyor shapes)

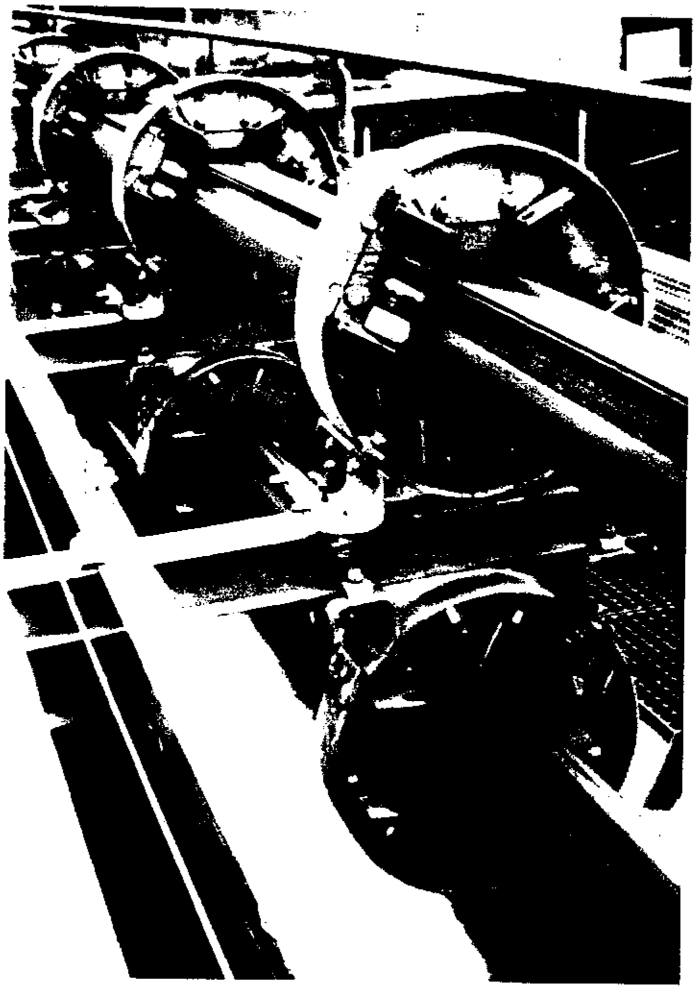

Fig. 2: "Rollgurt" Conveyor - Idler Configuration

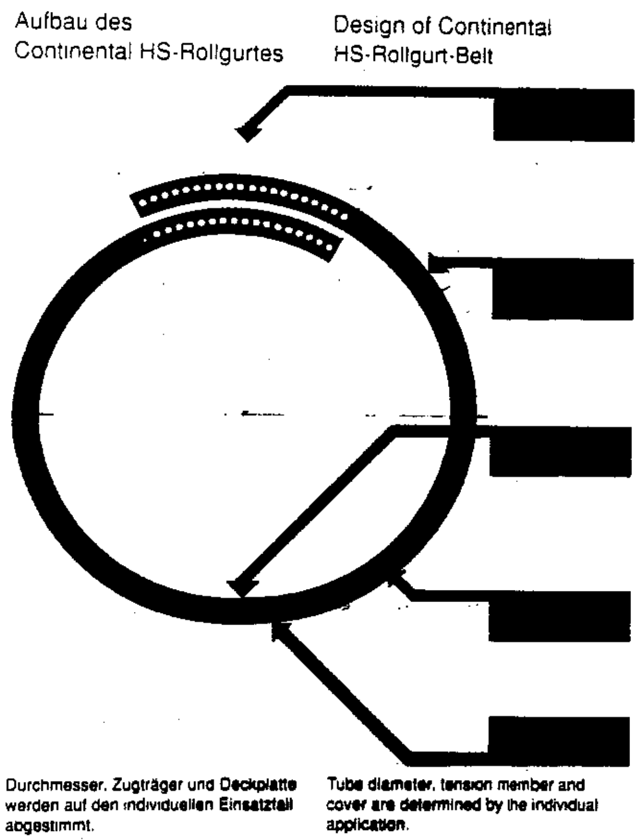


Fig. 3: Design of Continental HS-Rollgurt-Belt

Fig. 4: Curved Section of "Rollgurt" Conveyor

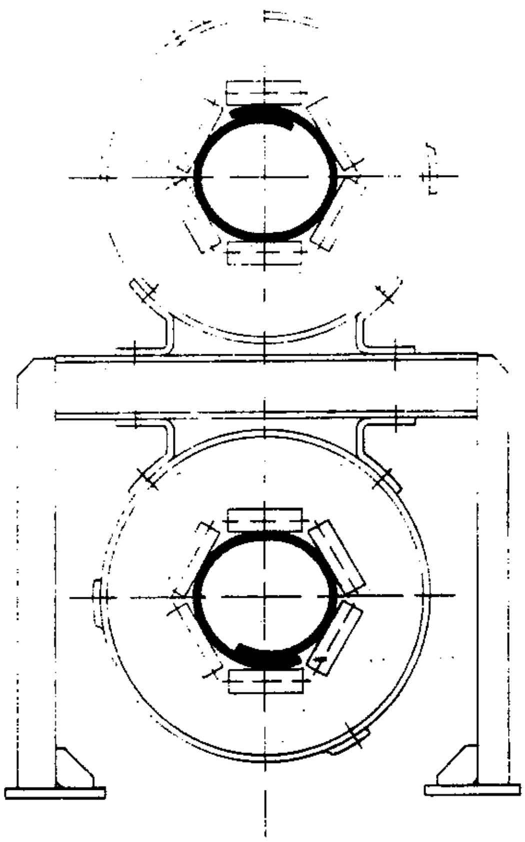

Querschnitt der Tragkonstruktion eines Rollgurtförderers

Cross-section of the support arrangement of a HS-Rollgurt-Conveyor

Fig. 5: Cross Section of the Support Arrangement of a HS-Rollgurt-Conveyor

Fig. 6: "Rollgurt" Conveyor Alsen-Breitenburg, Germany

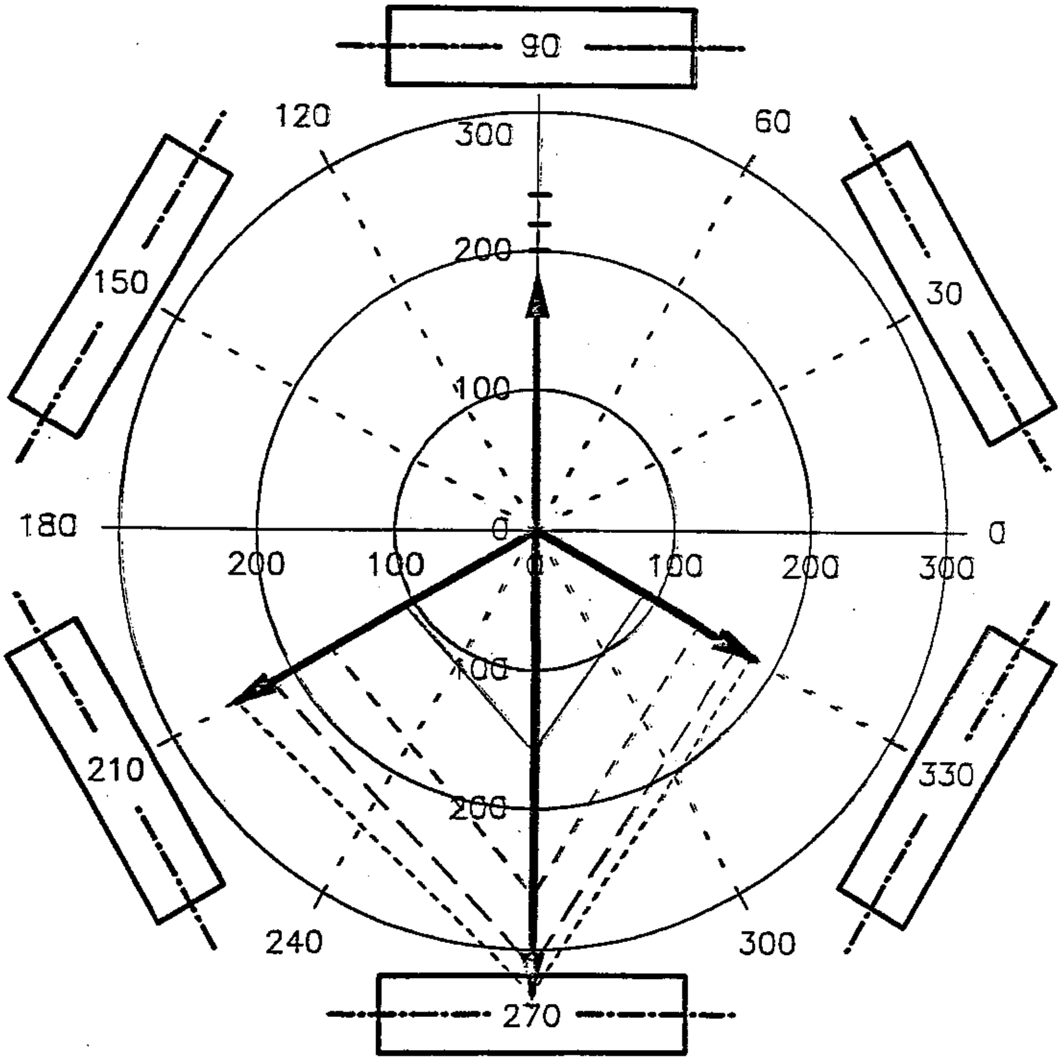


Fig. 7: Normalkräfte auf die Tragrollen an den verschiedenen Meßstellenpositionen

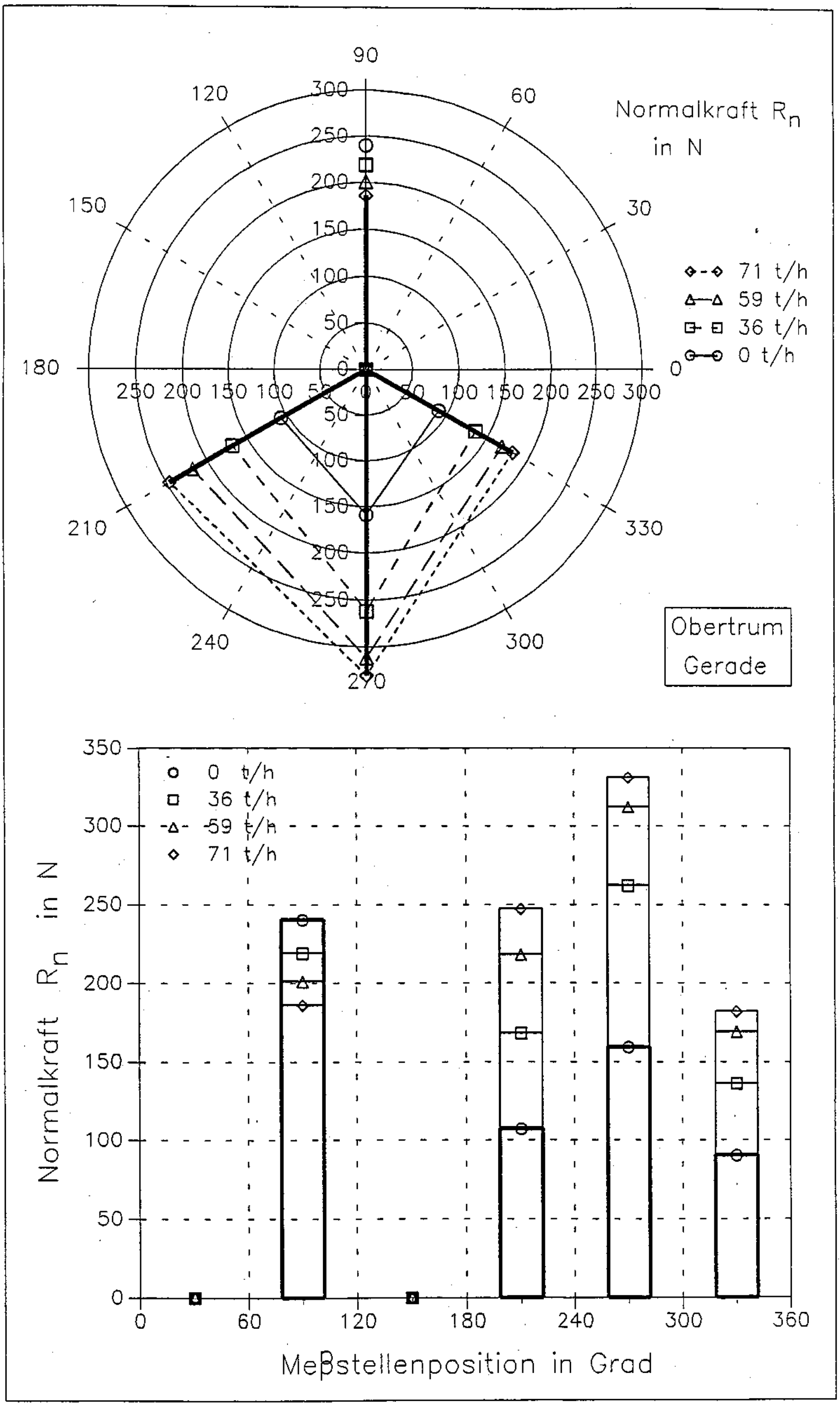

Normalkraft $R_n$ in N
90
120
60
150
30
180
0
210
330
240
300
270
71 t/h
59 t/h
36 t/h
0 t/h
Obertrum
Gerade
0 t/h
36 t/h
59 t/h
71 t/h
Normalkraft $R_n$ in N
Meßstellenposition in Grad


Fig. 8

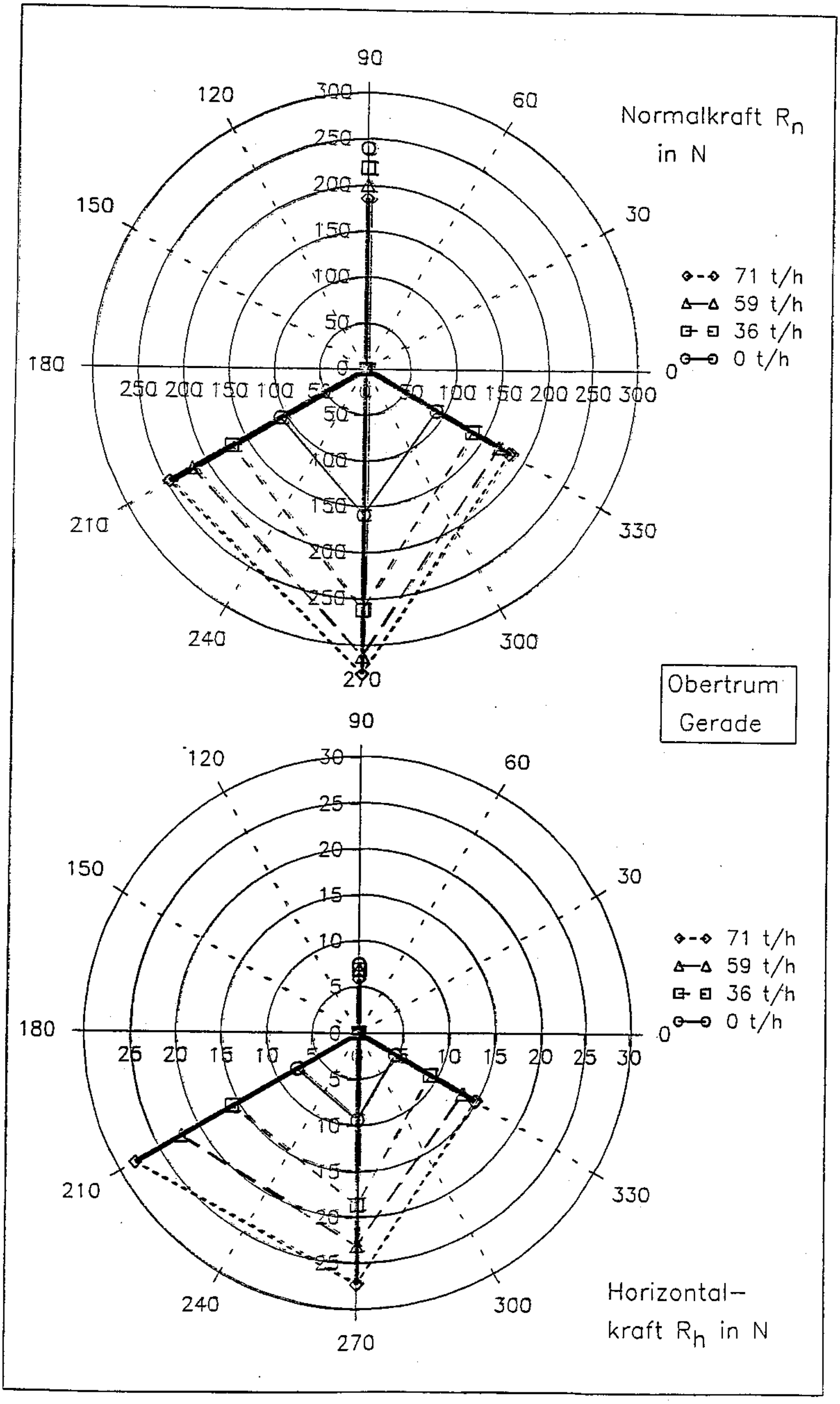
Normalkraft $R_n$ in N
71 t/h
59 t/h
36 t/h
0 t/h
Obertrum Gerade
Horizontal-kraft $R_h$ in N

Fig. 9

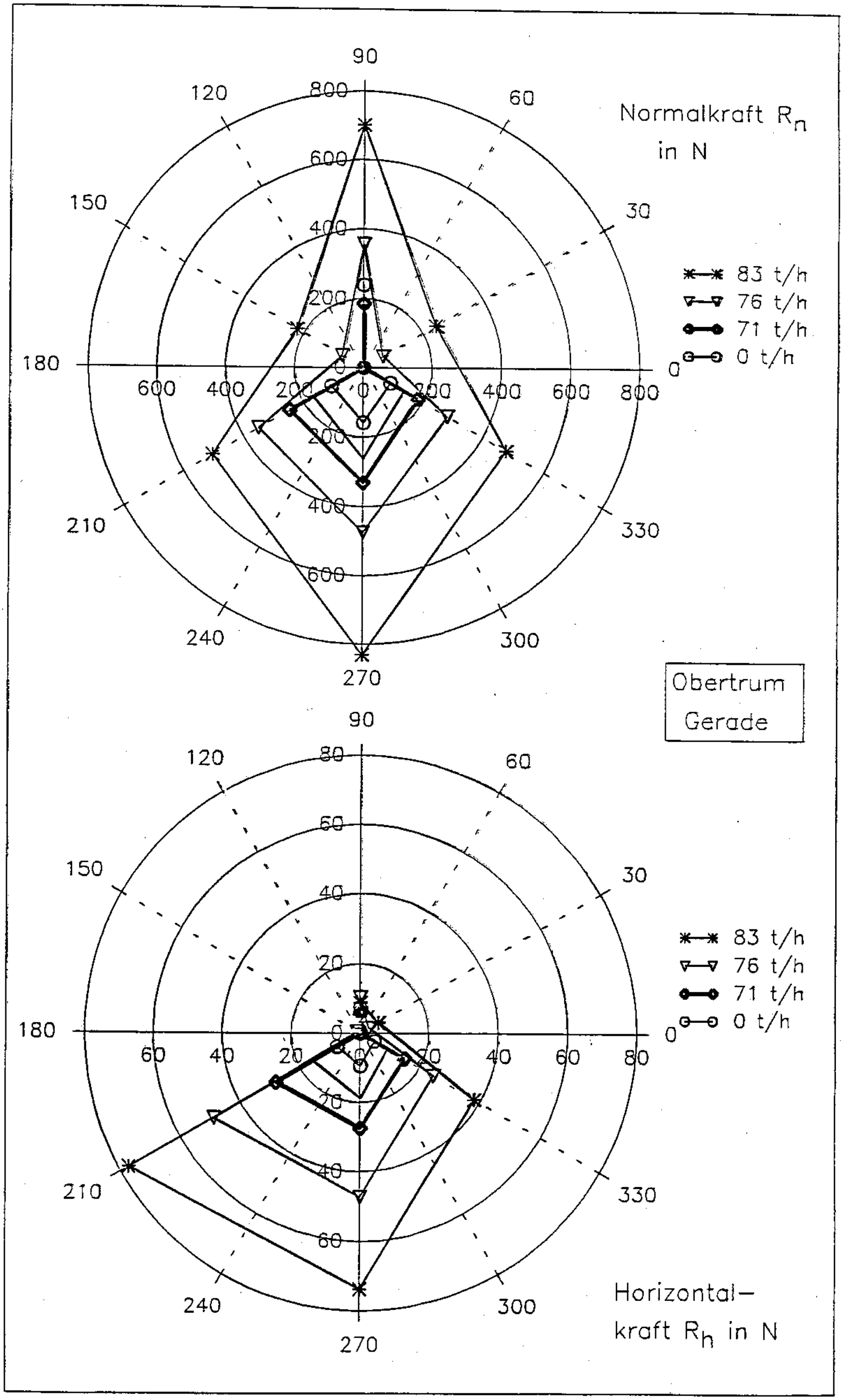
90
120
60
150
30
180
0
210
330
240
300
270
800
600
400
200
0
200
400
600
Normalkraft $R_n$ in N
83 t/h
76 t/h
71 t/h
0 t/h
Obertrum
Gerade
80
60
40
20
Horizontal-kraft $R_h$ in N

Fig. 10

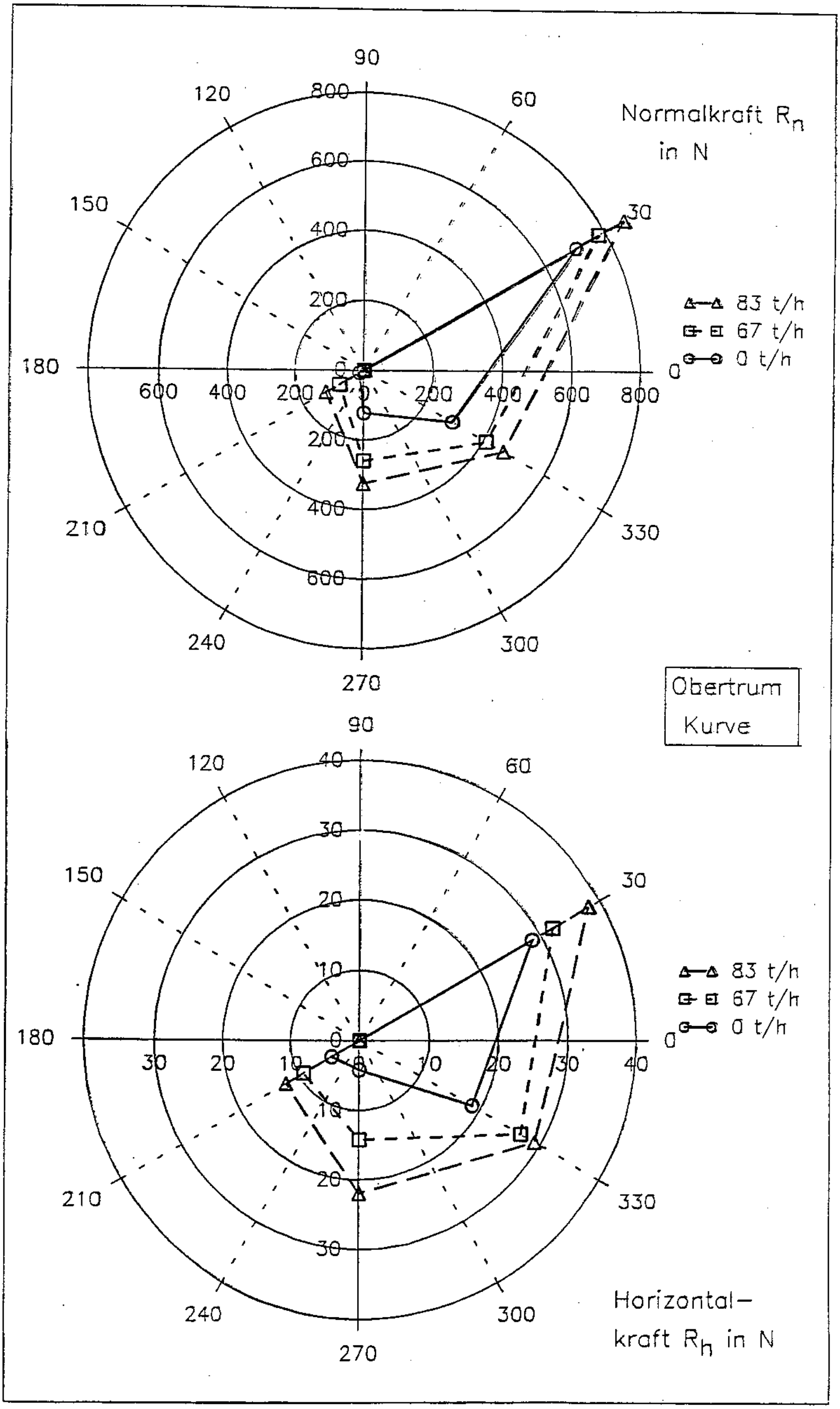
Normalkraft $R_n$ in N
83 t/h
67 t/h
0 t/h
90
60
30
0
330
300
270
240
210
180
150
120
Obertrum
Kurve
Horizontalkraft $R_h$ in N

Fig. 11

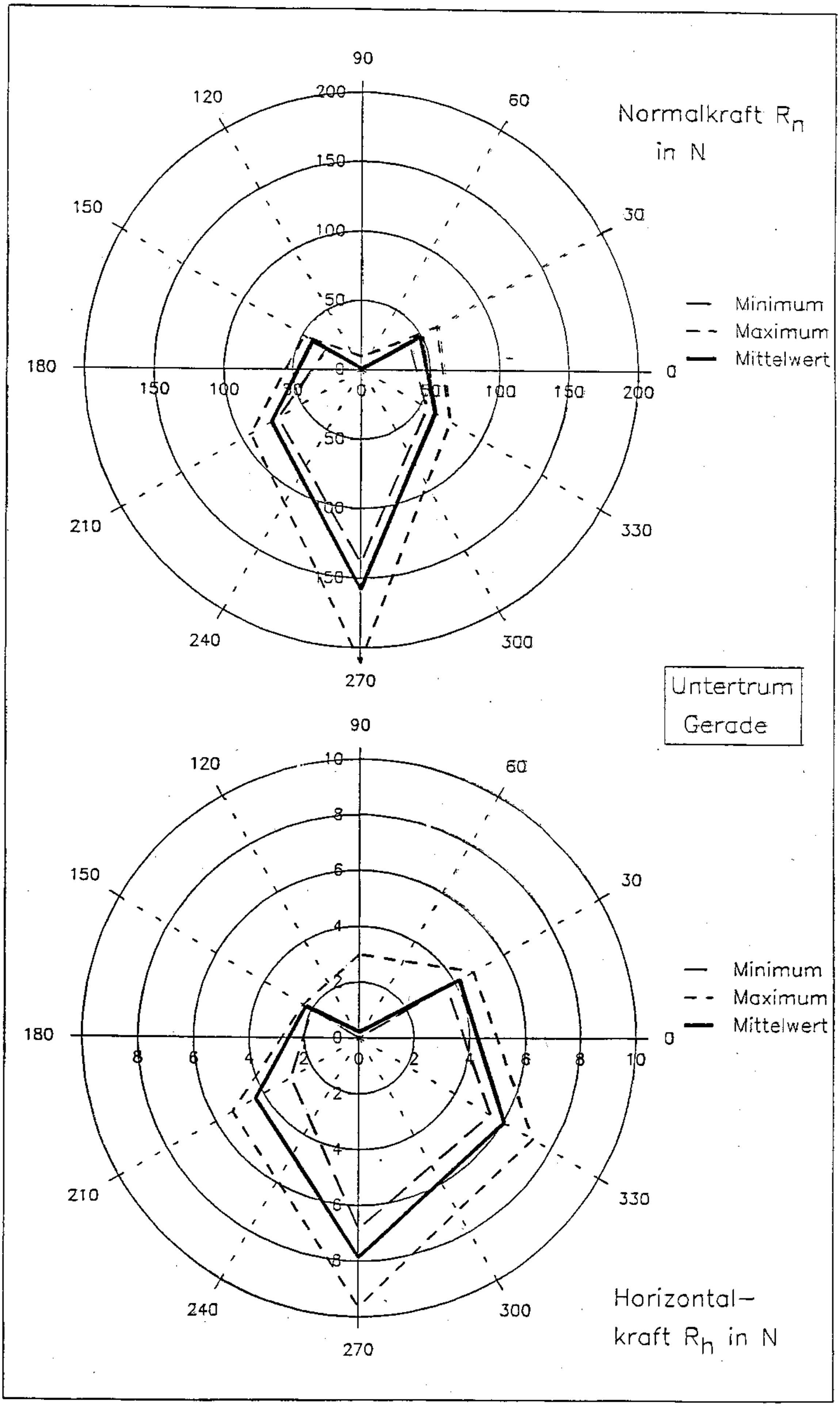
Normalkraft $R_n$ in N
Minimum
Maximum
Mittelwert
90
60
30
0
330
300
270
240
210
180
150
120
200
150
100
50
0
Untertrum
Gerade
Horizontalkraft $R_h$ in N
10
8
6
4
2

Fig. 12

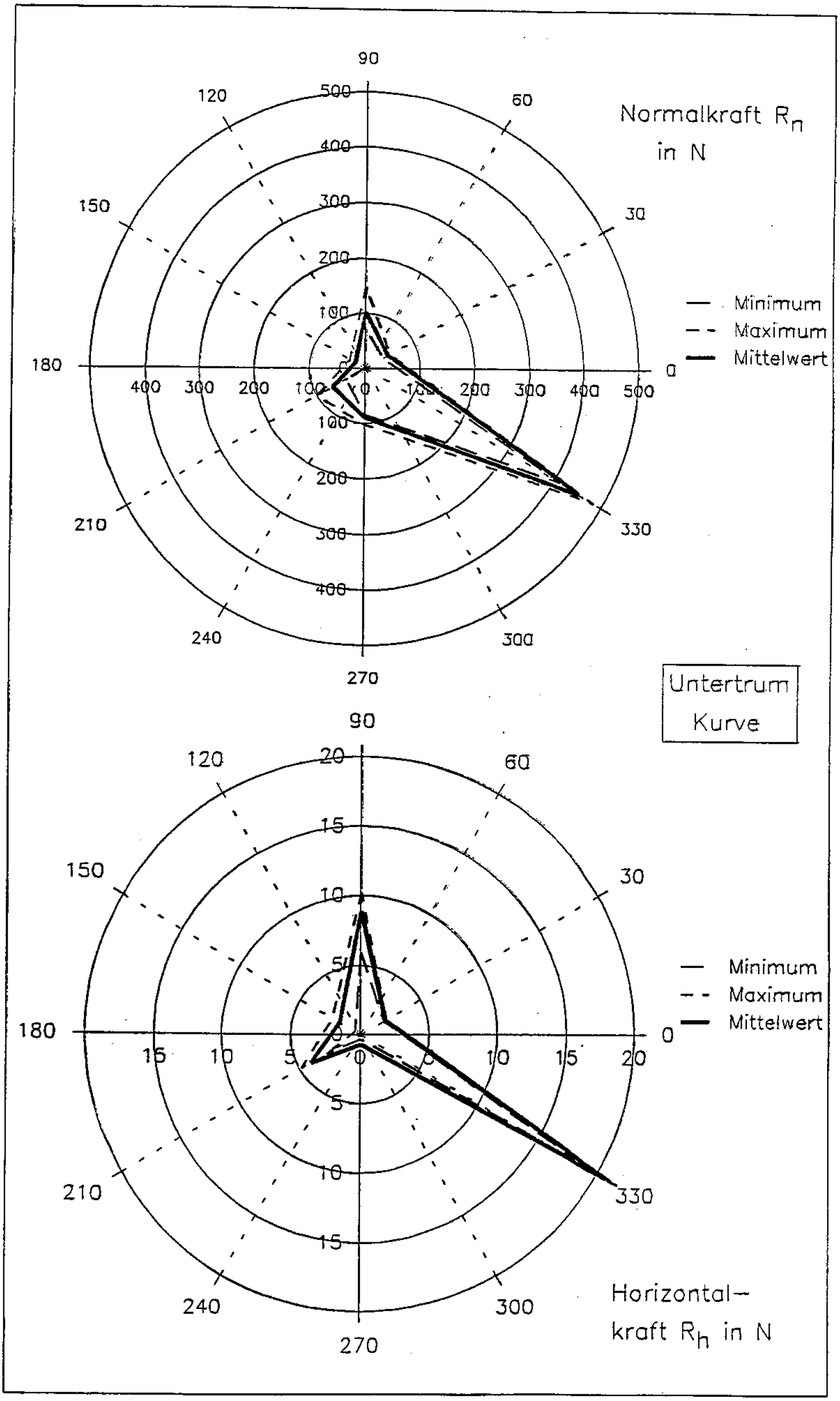
Normalkraft $R_n$ in N
Minimum
Maximum
Mittelwert
Untertrum
Kurve
Minimum
Maximum
Mittelwert
Horizontal-kraft $R_h$ in N

Fig. 13

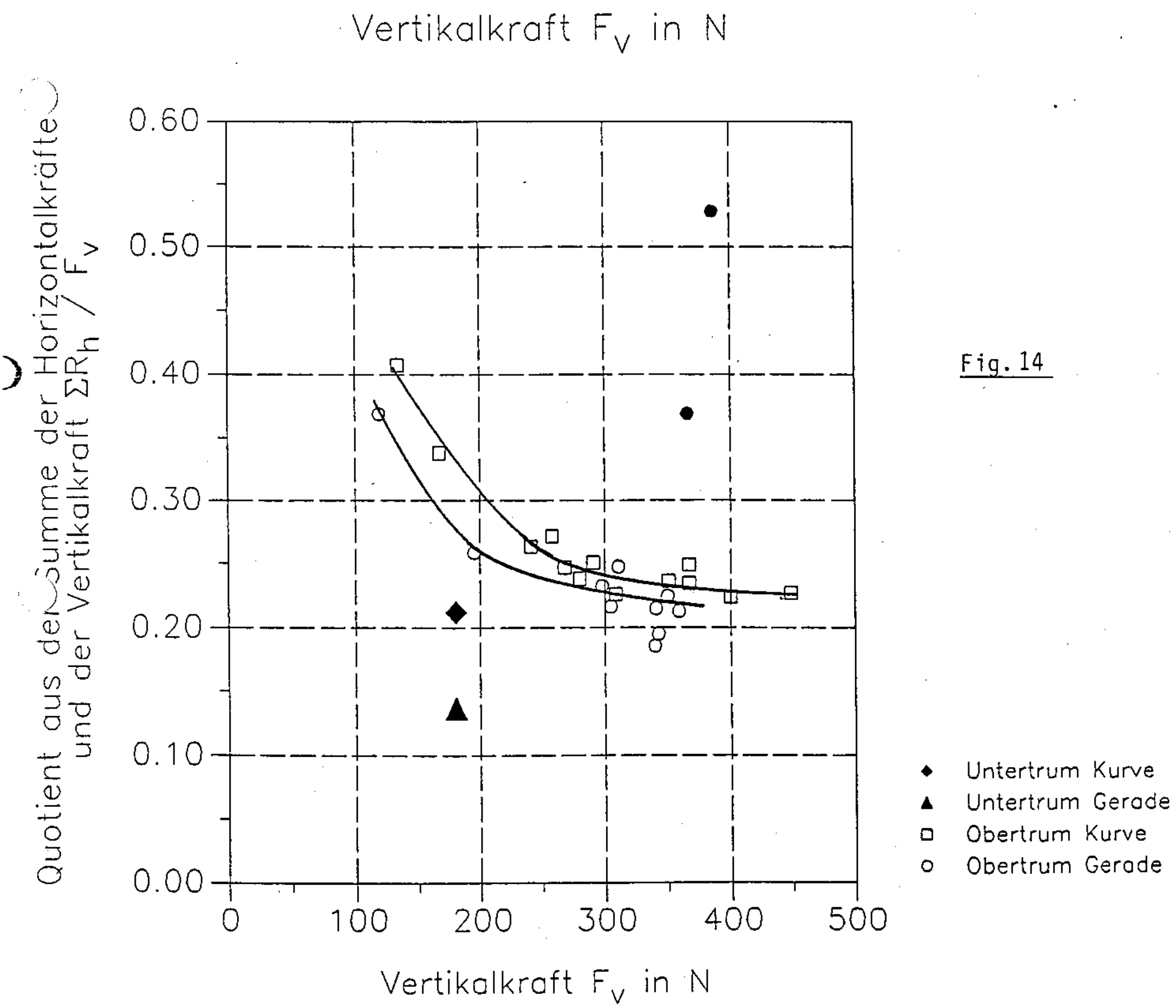

Vertikalkraft $F_V$ in N
Quotient aus der Summe der Horizontalkräfte und der Vertikalkraft $\Sigma R_h / F_V$
0.60
0.50
0.40
0.30
0.20
0.10
0.00
0
100
200
300
400
500
Vertikalkraft $F_V$ in N
Untertrum Kurve
Untertrum Gerade
Obertrum Kurve
Obertrum Gerade


Fig. 14

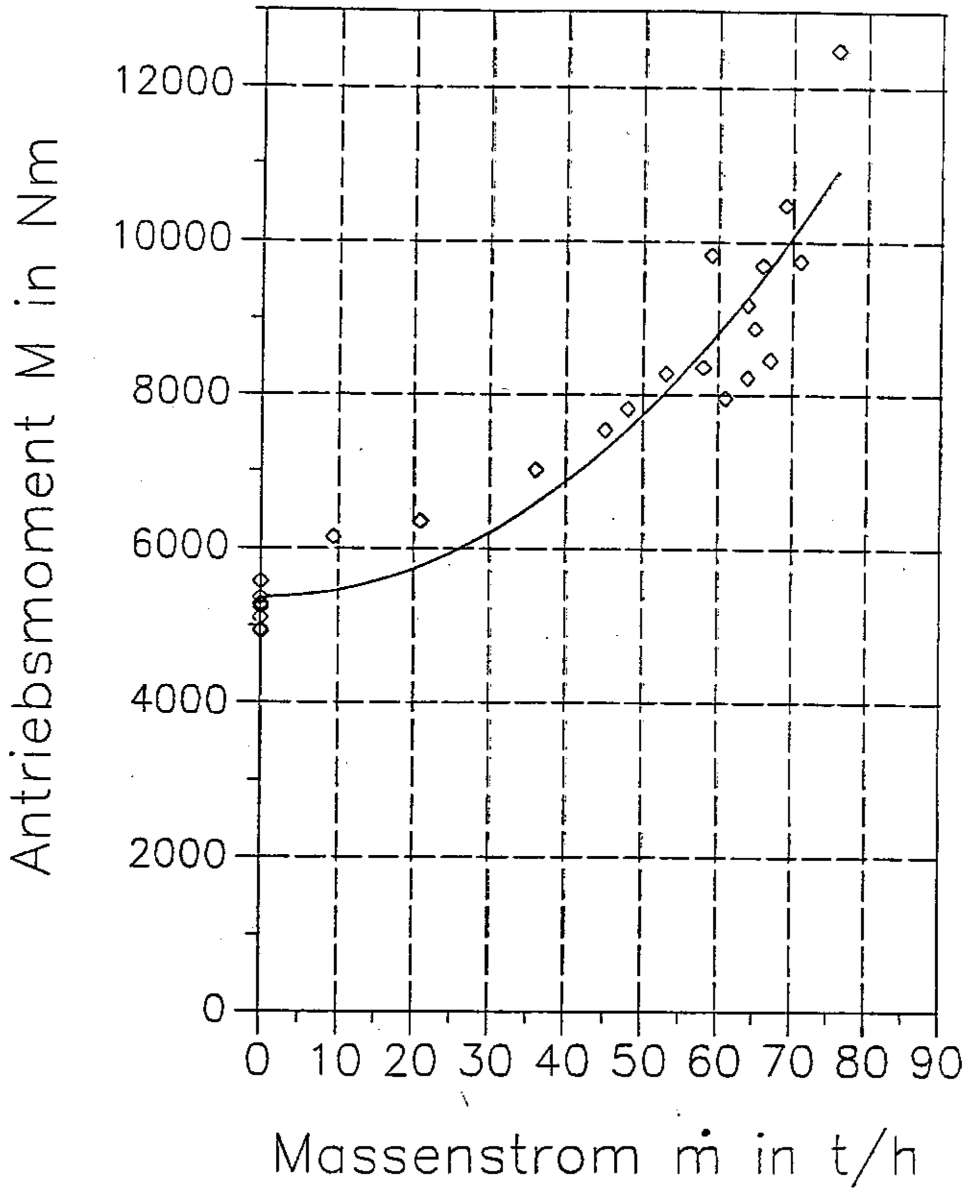
12000
10000
8000
6000
4000
2000
0
Antriebsmoment M in Nm
0
10
20
30
40
50
60
70
80
90
Massenstrom ṁ in t/h

Fig. 15

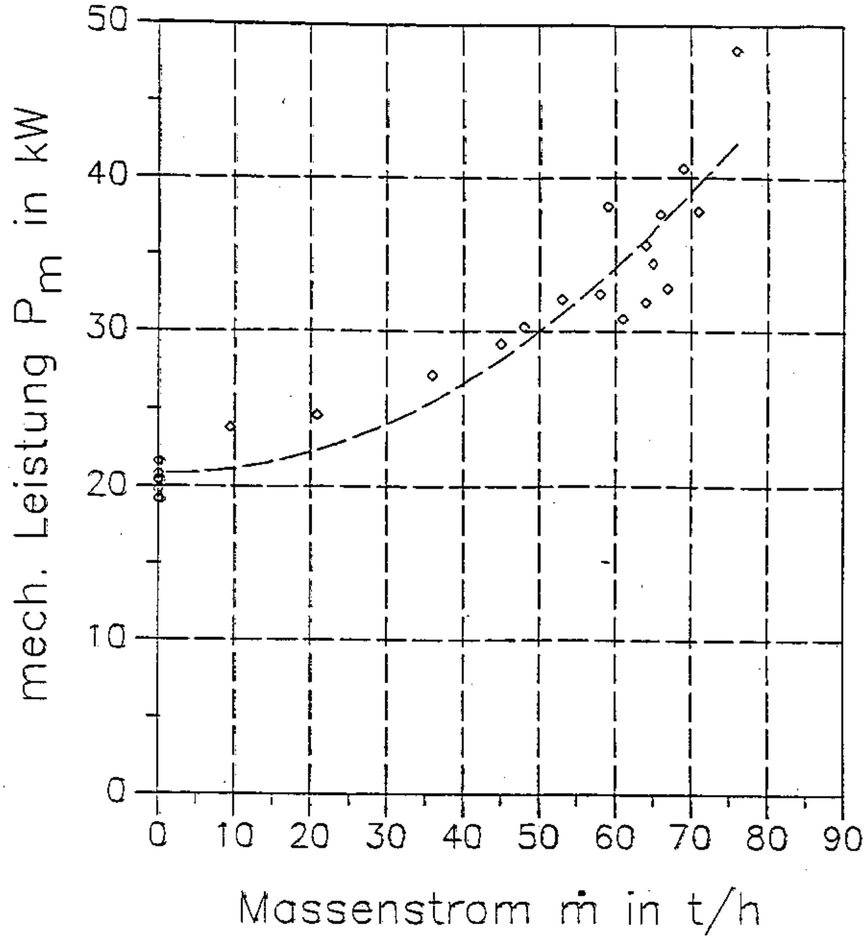

mech. Leistung $P_m$ in kW
0
10
20
30
40
50
0 10 20 30 40 50 60 70 80 90
Massenstrom $\dot{m}$ in t/h


Fig. 16

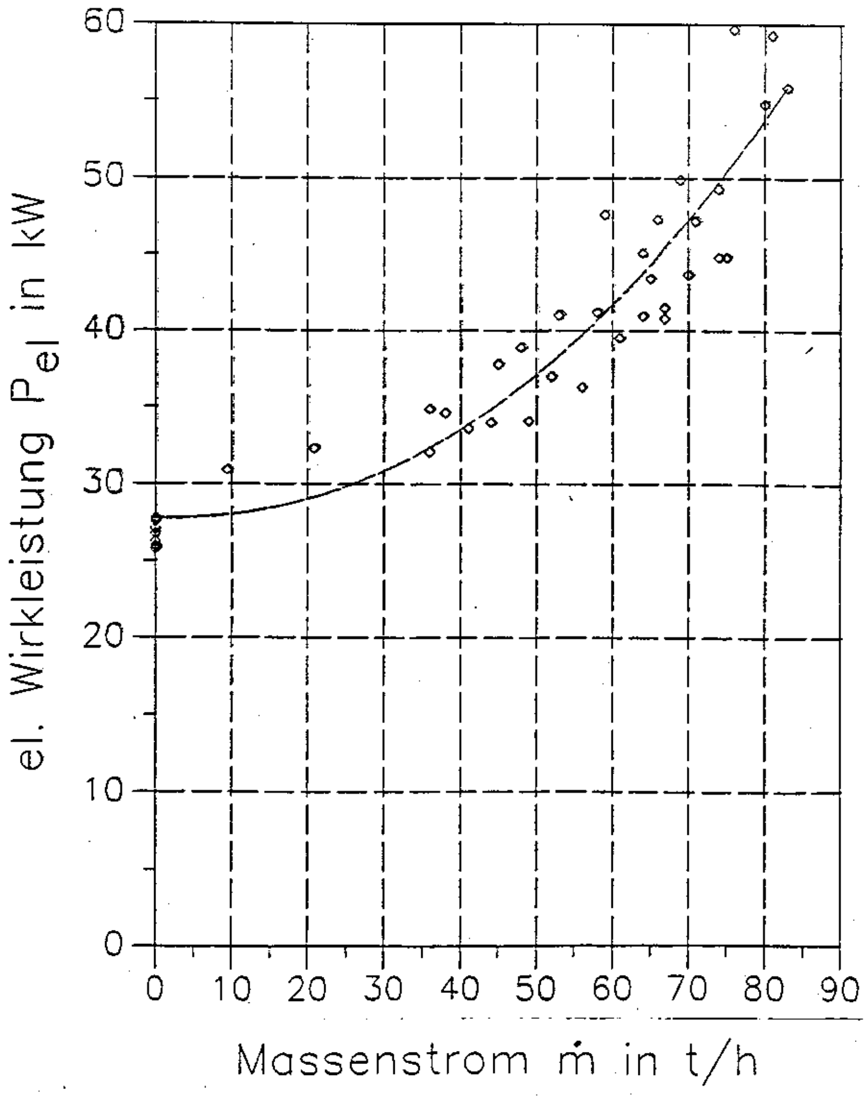

el. Wirkleistung $P_{el}$ in kW
0
10
20
30
40
50
60
0 10 20 30 40 50 60 70 80 90
Massenstrom $\dot{m}$ in t/h


Fig. 17

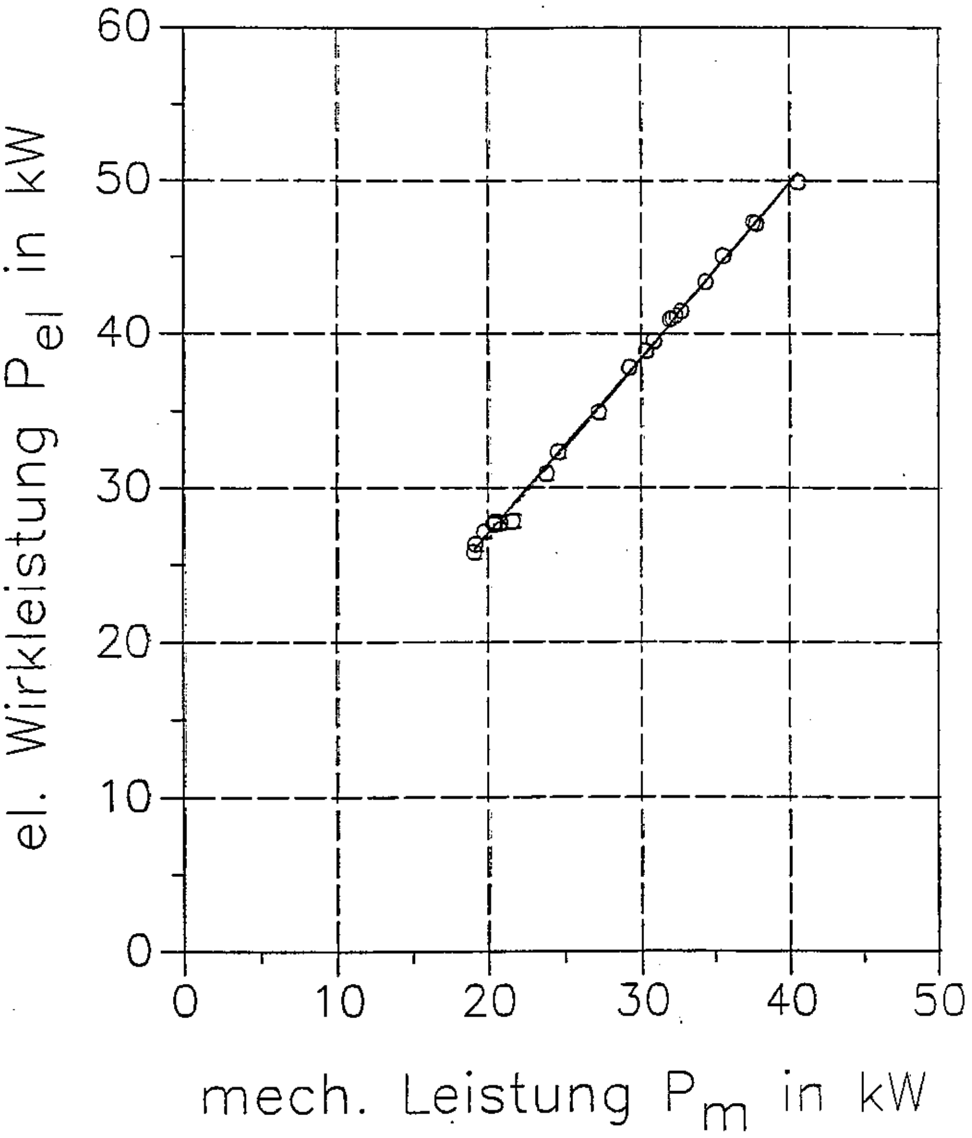
60
50
40
30
20
10
0
0
10
20
30
40
50
el. Wirkleistung $P_{el}$ in kW
mech. Leistung $P_m$ in kW

Fig. 18

Fig. 19

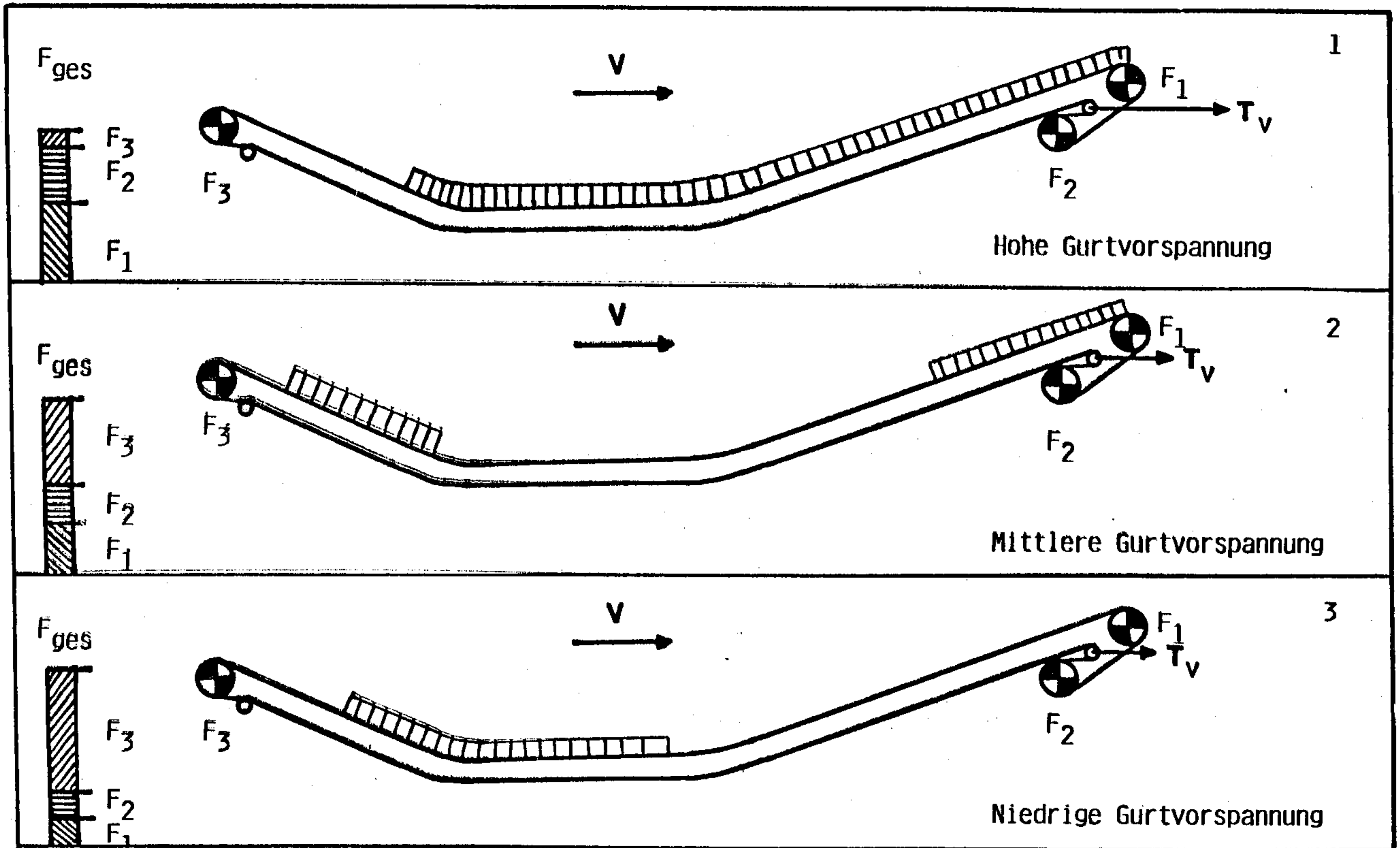


Anlagenwiderstand F = const bei unterschiedlichem
Reibungsbeiwert und Beladezustand

Fig. 20

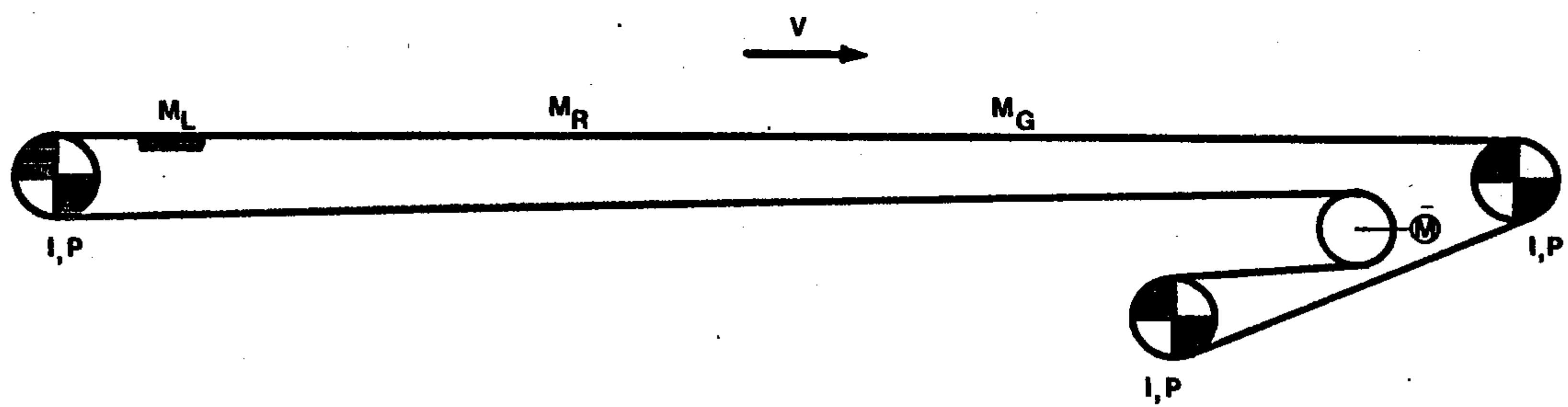


$$F = C \cdot f \cdot L \cdot (M_R + 2M_G + M_L) \cdot G \pm H \cdot M_L \cdot G$$

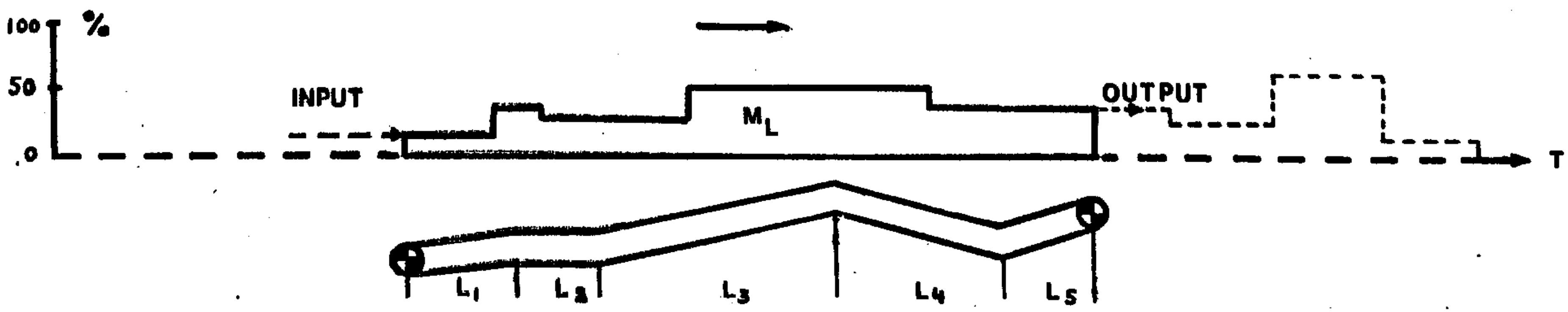


# CONVEYOR CONTROLS

BAHKE